European Journal of Orthodontics 19 (1997) 491–500

Superelastic nickel titanium alloy retraction springs—an experimental investigation of force systems

Christoph Bourauel*, Dieter Drescher*, Jan Ebling*, David Broome** and Andreas Kanarachos***

*Department of Orthodontics, University of Bonn, Germany, **Department of Mechanical Engineering, University College London, UK and ***Mechanical Design and Control Systems Section, National Technical University of Athens, Greece

SUMMARY The purpose of the present investigation was to study the mechanical characteristics of canine retraction springs made of superelastic nickel titanium (NiTi) alloys. A modified Burstone T-loop was used to construct an experimental canine retraction spring 10 mm in height and 10 mm in length. Twenty-five NiTi T-segments were hand made from the superelastic orthodontic alloys Ormco NiTi and Soar Sentalloy (dimensions 0.016 × 0.022″). The T-segments were equipped with arms made of rectangular standard steel wire (0.017 × 0.025″). The following geometrical and mechanical parameters of the retraction springs were analysed: radius and bending angles of the T-segments, distalizing force and M/F ratio during activation and the force/deflection rate of the springs. The error in the geometric parameters was in the range of 5–10 per cent, irrespective of the alloy used to produce the T-segments. On the other hand, the force systems of the springs were strongly influenced by the alloy and the batch under investigation. There were differences in the distalizing force of up to 100 per cent, i.e. at the beginning of the unloading plateau the distalizing force varied from 0.4 to 2.5 N. The force/deflection rate varied between a value of 0.06 and 0.15 N/mm, whereas the moment/force ratio reached values of 6.5–7.0 mm. Within a single batch, a reproducibility of these mechanical properties of approximately 5 per cent could be obtained. These results confirm that each orthodontic device made of superelastic NiTi alloys has to be calibrated individually. The manufacturers should pay more attention to keeping the material properties of their NiTi alloys constant.

Introduction

The most common aspects in the orthodontic treatment of extraction cases are the canine, the incisor and the en masse retraction. Depending on the techniques employed, a large number of different mechanisms are in use. A review of the literature gives several clinical (Smith and Storey, 1952; Bauer *et al.*, 1992; Bourauel *et al.*, 1993), experimental (Yang and Baldwin, 1974; Solonche *et al.*, 1977; Vanderby *et al.*, 1977; Koenig *et al.*, 1980; Gjessing, 1985, 1992; Drescher *et al.*, 1991; Bourauel *et al.*, 1992a) and numerical studies (Burstone and Koenig, 1974, 1976; Koenig and Burstone, 1974; DeFranco *et al.*, 1976; Greif *et al.*, 1982; Miyakawa *et al.*, 1985; Lippsett *et al.*, 1990; Bourauel *et al.*, 1992b, 1993) dealing with the force systems of fixed orthodontic devices and their clinical application. The numerical as well as the experimental studies are based on a two-tooth model developed by Burstone and Koenig (1974) and describe the behaviour of different retraction springs (T-shaped springs, U-loop, rectangular loop). These investigations were performed in an attempt to develop retraction mechanisms with optimal force systems.

A proper loop design, suitable for a canine or anterior retraction spring, has to fulfil the following requirements: the distalizing force should not exceed a maximum of about 2 N, while the spring has to deliver an antitip moment that ensures a bodily tooth movement. Depending on the treatment task, the necessary moment/force ratio (M/F) of 8–11 mm in the case of canine and anterior retraction,

respectively (Gjessing, 1985, 1992), can be calculated. Additionally, canine retraction requires a transversal moment/force ratio of a factor of about 4.5 mm.

The introduction of novel materials into orthodontic therapy offers the chance of further improvement in the effectiveness and reliability of orthodontic devices. Among these novel materials, the memory alloy nickel titanium NiTi (Buehler *et al.*, 1963) is one of the most promising. The use of nickel titanium wires in orthodontic treatment was first described by Andreasen and Hilleman (1971), Andreasen and Brady (1972) and Andreasen and Morrow (1978). Previous numerical and experimental investigations (Bourauel *et al.*, 1992b, 1993) led to the design of a T-loop made of a superelastic NiTi alloy that displayed favourable properties. This study presents the mechanical characteristics of this novel retraction spring and the experimental analysis of the force system, depending on the different orthodontic NiTi alloys used to construct the springs. The clinical application of the improved retraction spring has been demonstrated earlier (Bourauel *et al.*, 1993). Figure 1 displays the use of the NiTi T-loop in the case of the retraction of upper incisors.

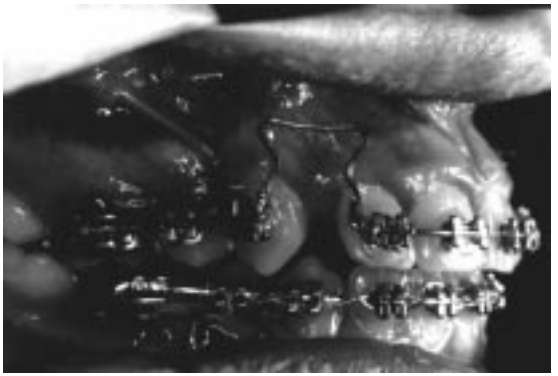

Figure 1 Retraction of upper incisors using a superelastic NiTi T-loop.

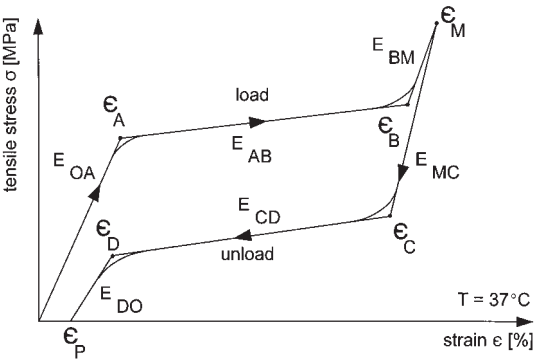

Figure 2 Definition of the parameters of superelasticity. It is necessary to distinguish between a loading and an unloading branch.

Superelastic NiTi alloys

The mechanical properties of nickel titanium alloys are characterized by the memory effect (Buehler *et al.*, 1963; Andreasen *et al.*, 1979) and the so-called pseudo- or superelastic behaviour (Miura *et al.*, 1986). Figure 2 displays the schematic stress/strain diagram of a superelastic NiTi alloy. It results from a uni-axial tensile test and shows an extreme non-linearity.

An increase in strain up to a value of ε_A results in a linear increase in stress. A non-linear regime around ε_A is followed by the superelastic plateau that is characterized by a wide range of strain (ε_A–ε_B) with nearly no ascent in stress. The yield strength (ε_M) of NiTi alloys may reach values of about 8 per cent. Unloading the material results in a wide hysteresis, as the parameters have changed slightly. Consequently, it is necessary to distinguish between a loading and an unloading branch. The parameters defined in Figure 2 depend on the composition of the alloy investigated and are in the following range:

E_{OA} and E_{DO}:	20 kN/mm^2 up to 60 kN/mm^2
E_{AB} and E_{CD}:	0.1 kN/mm^2 up to 5 kN/mm^2
E_{BM} and E_{MC}:	10 kN/mm^2 up to 30 kN/mm^2
ε_A and ε_D:	0.5 per cent to 2.5 per cent
ε_B:	5.0 per cent to 8.0 per cent

The strain limit ε_C depends on the loading history and is not a parameter characteristic of a certain NiTi wire. Therefore, this parameter was not analysed in the course of this study. As the elastic properties of NiTi wires are extremely sensitive to a change in temperature, the tensile test has to be conducted at 37°C, the application temperature of orthodontic NiTi wires.

Superelasticity is the most favourable behaviour of the NiTi alloys, as it allows the construction of orthodontic devices with exceptional properties. These result from the very low modulus of elasticity, a yield strength of about 8 per cent and the typical hysteresis loop of NiTi alloys. Consequently, superelastic retraction springs deliver the following characteristics:

- nearly constant forces and moments over a broad range of activation, if the superelastic plateau is reached;
- very low distalizing forces;
- very low force/deflection rates;
- a proper loop design ensures a nearly constant moment/force ratio over several millimetres of activation;
- the danger of exceeding the biological or physiological limits is minimized, as the force of activation will rise dramatically, when the superelastic plateau is left;
- unloading the loop leads to a still lower distalizing force, as the NiTi alloy is on the unloading branch;
- this load mode corresponds to the clinical application, as a retraction spring is first activated and then, during the orthodontic tooth movement, deactivated.

Materials and methods

Superelastic T-loop

Burstone and Koenig (1976) calculated the force systems of different retraction springs. They used the alloy TMA to construct a T-loop that has a sagittal moment/force ratio of about 9 mm and a distalizing force between 1.0 and 2.0 N. The *M*/*F* ratio of this loop is not constant over a retraction path of 3 mm, but varies from 7 to 11 mm. Therefore, numerical as well as experimental studies were performed to construct a novel retraction spring based on an improved Burstone T-loop. This T-loop makes use of the superelastic properties of NiTi alloys and has a nearly constant force system over a broad range of activation (Bourauel *et al.*, 1993). Figure 3a shows a superelastic retraction spring resulting from these investigations. The retraction spring consists of a T-segment made of different superelastic orthodontic NiTi alloys. These T-segments are connected to arms made of a stainless steel wire (3M Unitek, Monrovia, CA 91740-5339) via crimpable hooks, to form a T-shaped retraction loop.

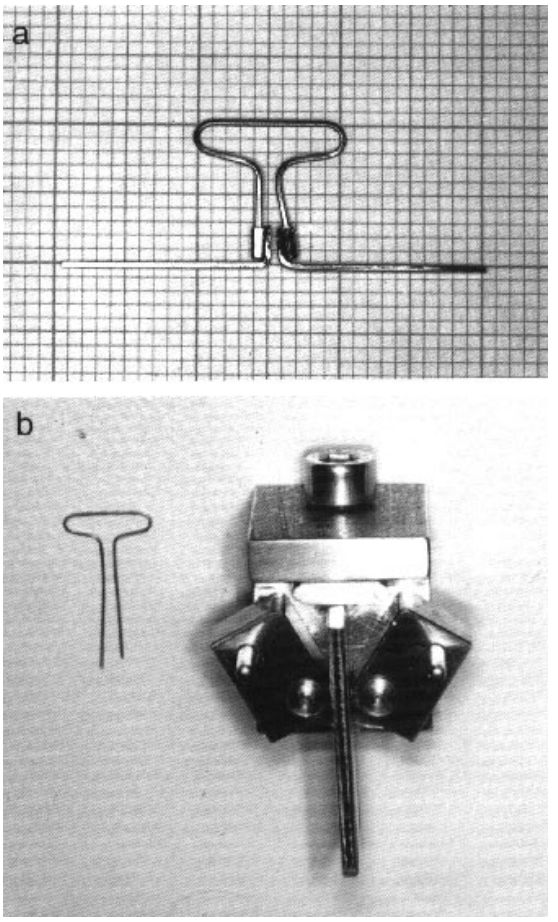

Figure 3 (a) Composite retraction spring made of a NiTi T-segment and stainless steel arms. The steel arms are connected via crimpable hooks to the NiTi-segment. (b) Device to produce NiTi T-segments. Different orthodontic NiTi wires are inserted into the device and are heat treated for 3 hours at a temperature of about 300°C.

As it is impossible to bend NiTi alloys with pliers, the T-segments were produced by heat treating the wires in an oven. Figure 3b shows the experimental device used to perform the heat treatment. Straight sections of different NiTi wires were inserted into the device and after a heat treatment for 3 hours at a temperature of approximately 300°C, the NiTi T-segments were

taken out and combined to the T-shaped retraction springs. Subsequently, the geometric parameters and the force systems of the T-loops were measured with reference to the NiTi wire used. Figure 4a gives the geometric parameters of the T-segments (radius of the T-segment: r_T; angle of T: α_T; angle of the legs: α_L; angle of divergence: α_D). The former investigations established a loop design of a height and length of 10 mm each and the following geometric parameters: r_T = 1 mm, α_T = 180 degrees, α_L =90 degrees, no divergence of the legs. In Figure 4b, the dominant components of the measured force system (distalizing force *F*, uprighting moment *M*) are displayed. Mechanical and geometrical parameters are used to characterize the mechanical behaviour of the springs as well as the geometrical properties of the heat-treated NiTi wire.

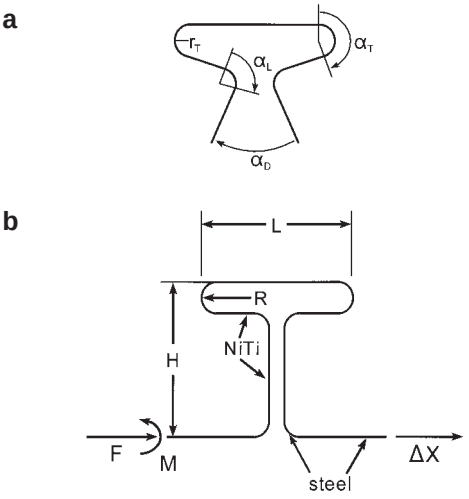

Figure 4 (a) Definition of the geometric parameters of the NiTi T-segment, investigated in this study. (b) Dominant components of the force system of a retraction spring that is activated.

Orthodontic NiTi wires

The T-segments were produced from two different superelastic orthodontic NiTi alloys and four different batches of the one wire. The elasticity parameters of Ormco NiTi (Ormco Corporation, 1332 South Lone Hill Avenue, Glendora, CA 91740-5339) and Sentalloy NiTi (GAC International Inc., 185 Oval Drive, Central Islip, NY 11722) are listed in Table 1. The parameters are defined according to Figure 2 and are derived from an improved bending test in combination with a planar theory of superelastic behaviour (Plietsch *et al.*, 1994). Both Ormco NiTi and Sentalloy NiTi display distinct superelastic behaviour. On the other hand, the parameters differ significantly. The parameters ε_A and ε_D are of utmost importance, as they define the point where the alloys enter and leave the superelastic plateau. A low value in the strain limit ε_D results in a low stress on the

Table 1 Parameters of superelasticity for the alloys used during this study (ambient temperature 37°C).

	Parameter (E in kN/mm^2; ε in %)									
	E_{OA}	E_{AB}	E_{BM}	E_{DO}	E_{CD}	E_{MC}	ε_A	ε_B	ε_D	ε_P
Ormco NiTi batch 2A 188A	56.5 (8)	0.14 (5)	19.2 (7)	39.6 (3)	0.33 (8)	29.4 (9)	0.96 (4)	5.1 (2)	0.54 (1)	0.31 (2)
Sentalloy NiTi batch 4126	55.5 (7)	0.23 (4)	22.1 (9)	*	1.3 (2)	22.4 (9)	0.45 (2)	5.5 (1)	*	0.50 (10)
Sentalloy NiTi batch 0936	53.5 (9)	0.28 (6)	23.1 (7)	46.1 (3)	0.9 (5)	26.1 (1.5)	0.53 (2)	5.1 (1)	0.48 (1)	0.39 (5)
Sentalloy NiTi batch 3511	54.5 (9)	0.21 (4)	26.1 (9)	42.9 (7)	1.5 (2)	25.9 (2.1)	0.57 (3)	5.2 (1)	0.54 (2)	0.41 (7)
Sentalloy NiTi batch 9116	57.5 (9)	0.24 (5)	24.1 (9)	45.1 (4)	1.3 (5)	25.4 (2.0)	0.73 (2)	5.3 (1)	0.28 (1)	0.11 (1)

The parameters are derived from a bending test and are defined according to Figure 2. Mean from five measurements. The value in parentheses gives the error in the last places.
*Unable to determine E_{BM} and ε_D due to strong martensitic deformations.

plateau upon unloading. Therefore, ε_P must be substracted from ε_D to calculate the strain determining the stress on the plateau. For example, in the case of Ormco NiTi, the following values result: ε_D = 0.54 per cent and ε_P= 0.31 per cent. This results in a strain of ε = 0.23 per cent. As this value determines the mechanical behaviour of the retraction springs, a small value in ε_D would give a small distalizing force (Bourauel *et al.*, 1993). On the other hand, if this parameter is too small or approaches a value of 0 per cent, then, due to martensitic deformation, the spring would not reach the initial state and would remain deformed after activation. The batch 4126 of Sentalloy displays this behaviour.

From each NiTi wire, five T-segments were produced, giving a total of 25 NiTi T-loops. The angles and radii of the loops were determined and the force systems were measured. For each loop, the mean and standard deviations of these values were calculated individually.

Experimental set-up

The experimental studies were performed using the Orthodontic Measurement and Simulation System (OMSS). Technical details and the application of the OMSS in orthodontics have been described in detail earlier (Drescher *et al.*, 1991; Bourauel *et al.*, 1992a). Figure 5a shows a schematic diagram of the components of the OMSS, and Figure 5b a photograph of the experimental set-up. The OMSS consists of the following major components:

- personal computer running the control software;
- force-torque transducer and six axes positioning table N° 1;
- force-torque transducer and six axes positioning table N° 2;
- temperature-controlled chamber, to ensure experimentation in a constant-temperature environment (37°C).

Both the force-torque sensors and the positioning tables are divided into a mechanical and an electronic part. Each subsystem is computer controlled by its own single-board microcomputer. The whole set of five computers is connected by a local area network based on the RS232 interface. Specifics of the force-torque tranducers are summarized in Table 2; the accuracy of the positioning tables is in the range of 10 μm and 0.1 degree, respectively.

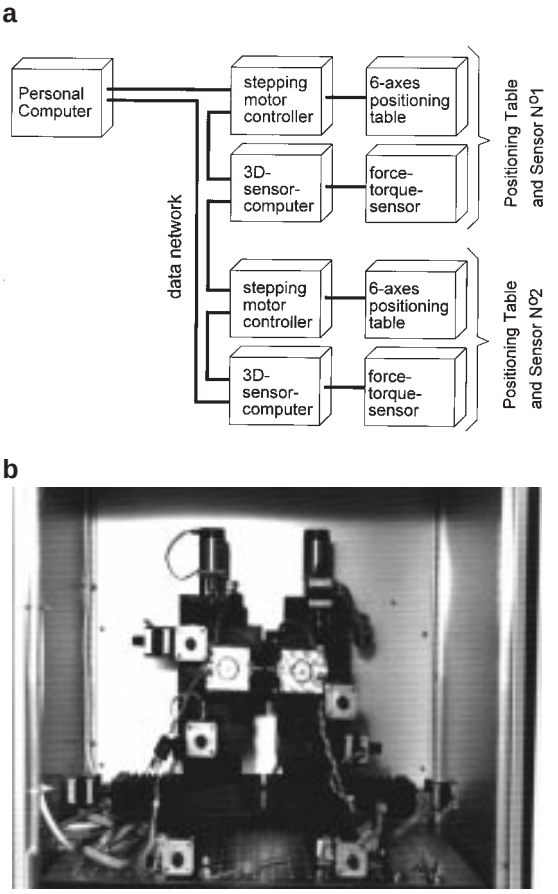

Figure 5 The measurements were performed using the Orthodontic Measurement and Simulation System [(a) schematic diagram; (b) photograph of the experimental set-up]. The OMSS provides full three-dimensional calibration and simulation measurements of orthodontic devices.

Table 2 Specifics of the force–torque transducers.

Simultaneous registration of three forces and three torques	
Forces: measuring range (resolution)	± 15.00 (0.02) N
Torques: measuring range (resolution)	± 450.0 (0.5) N
Maximum error in linearity and cross talk	0.3%
Physical dimensions	60 × 60 × 60 mm^3

The OMSS provides different measurement methods which enable the calibration of orthodontic appliances by a movement of the positioning tables along a specified path or by a combined variation of single or multiple axes (Drescher *et al.*, 1991). The system simultaneously records the three forces and three moments generated by the appliance. The most common type of measurement is the registration of a force/deflection diagram. Besides these calibration measurements, a simulation of orthodontic tooth movements is realized, i.e. repeatedly measuring the force system of an appliance, calculating the resulting tooth movement based on a mathematical model and conducting the motions by means of the computer-controlled positioning stages.

Results

Loop geometry

In Table 3, the results of the measurements of the loop geometry are listed. As there was no influence of the NiTi wire or batch used, all 25 T-segments were analysed in common. An error of about 5–10 per cent was obtained for the different parameters, which is in the range of hand-made springs. The variation in loop geometry is the same from loop to loop as from one batch to another.

Force system

Figure 6 depicts the influence of the different alloys and batches on the force system of the superelastic T-loop. The force/activation curves reflect the different parameters of the wires given in Table 1. The T-loop made from the alloy Ormco (marked as 1) delivers the highest distalizing force, whereas the superelastic plateau on the unloading branch of the Sentalloy T-loop (batch 4126, marked no. 4) crosses the x-axis. The curves of the other batches of the Sentalloy wire pass in between these two extremes. This behaviour coincides with the fact that the strain limits ε_A and ε_D of the Ormco wire are the highest, while the parameters of the Sentalloy wires decrease in the following order: batches 9116–3511–0936. As batch 4126 of the Sentalloy wire undergoes significant martensitic deformation (ε_D and ε_P are of the same order of magnitude), the unloading branch does not cross the origin. On the other hand, the elastic moduli of the five NiTi wires differ only slightly. These facts confirm the assumption that the force systems of superelastic retraction springs are dominated by the strain limits ε_A and ε_D.

Table 3 Geometric parameters of the experimental T-loops.

	Radius of T (r_T) (mm)	Angle of T (α_T)	Angle of legs (α_L)	Angle of divergence (α_D) (°)
Mean	1.29	164	98	16
SD	0.05	3	1	2

There was no influence of the batch under investigation on the geometry of the superelastic retraction spring.

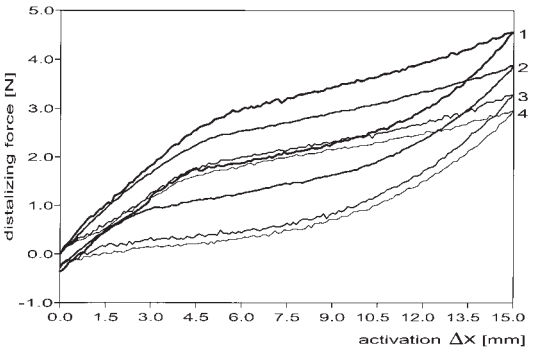

Figure 6 Comparison of the distalizing force F of four superelastic T-loops. The influence of the different alloys and batches is quite obvious (1 = Ormco NiTi, others: Sentalloy, 2 = batch 9116, 3 = batch 3511, 4 = batch 4126).

Figure 7a shows the force/activation curve of three subsequently produced NiTi T-loops (Sentalloy NiTi, batch 9116). Two curves nearly coincide completely, and the third one gives the maximum variation in distalizing force within T-loops produced from one batch. The plateau starts on the loading branch at a force of $F = 2.4$ N and, due to geometrical non-linearities, it rises to a value of about $F = 3.2$ N. At an activation of $X = 12$ mm, the second linear elastic regime starts. On the plateau of the unloading branch, the distalizing force decreases from about 1.7 N (activation $X = 10.5$ mm) to 0.8 N ($X = 3.5$ mm). This gives a force/deflection rate of about 0.13

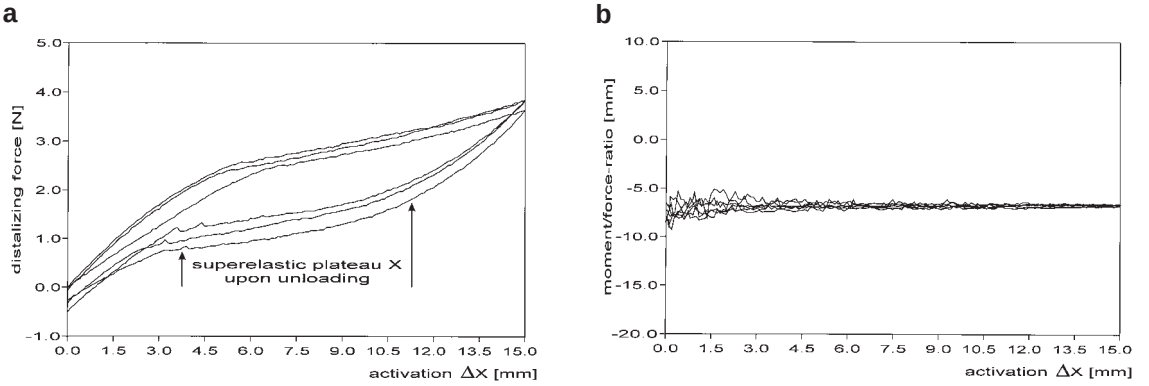

Figure 7 The force systems of three subsequently produced NiTi T-loops (Sentalloy Superelastic Nickel Titanium Alloy, batch 9116). (a) Force/activation curve. (b) Example of the measured activation curve of the *M*/*F* ratio.

Table 4 Distalizing force *F*, moment/force ratio *M*/*F* and force/deflection rate *F*/*X* on the superelastic plateau of the T-loops.

Parameter	Distalizing force *F* (N)	Moment/force ratio (mm)	Force/deflection rate (N/mm)	Plateau (mm)
Ormco NiTi batch 2A 188A	1.50–2.54 (8)	6.7 (3)	0.149 (2)	4–11
Sentalloy NiTi batch 4126	0.00–0.40 (10)	6.8 (2)	0.060 (20)	0–7*
Sentalloy NiTi batch 0936	0.10–0.87 (4)	7.0 (1)	0.096 (12)	3–11
Sentalloy NiTi batch 3511	0.10–0.95 (10)	6.5 (1)	0.106 (24)	3–11
Sentalloy NiTi batch 9116	0.90–1.73 (12)	7.0 (1)	0.129 (9)	5–12

All parameters are measured upon unloading. The last column gives the range *X* of the plateau.
*Strong martensitic deformation of the spring, start of the plateau cannot be determined.

N/mm, which is an excellent value for a retraction spring. As in Figure 6, the maximum activation of the T-loops is about $X = 15$ mm. The *M*/*F* ratio of the superelastic T-loop (Figure 7b) is nearly constant over the complete activation/deactivation cycle with a value of approximately 7 mm. This is about 1 mm too small for retraction of the canine. The ratio may be increased by a variation of the height of the steel segments and thus adapted to the requirements of retraction mechanics.

In Table 4, the parameters of all T-loops, produced from the different NiTi wires, are listed. From this table, it is quite obvious that the mechanical parameters of the NiTi wires have only a minor influence on the *M*/*F* ratio of the spring. The *M*/*F* ratio only varies from 6.5 to 7.0 mm between the different T-loops. On the other hand, there is a strong dependency of the distalizing force on the wire used. While the distalizing force of the Ormco loop is a little too high (1.50–2.54 N), some batches of the Sentalloy wire seem to result in superelastic T-loops, that are not suitable for a retraction spring. Distalizing forces below a value of 0.5 N seem to be too small for retraction springs.

In Figure 7a, the widths of the plateaus on the unloading branch are marked. From Table 4, it can be seen that this value depends on the alloy used. The range of the plateaus nearly coincides with all alloys used (7–8 mm), but the starting points vary significantly (0–5 mm), as they are determined by the strain limits ε_D and thus directly reflect the behaviour of the alloy used. From the width of the plateaus, together with the distalizing forces, the very low force/deflection

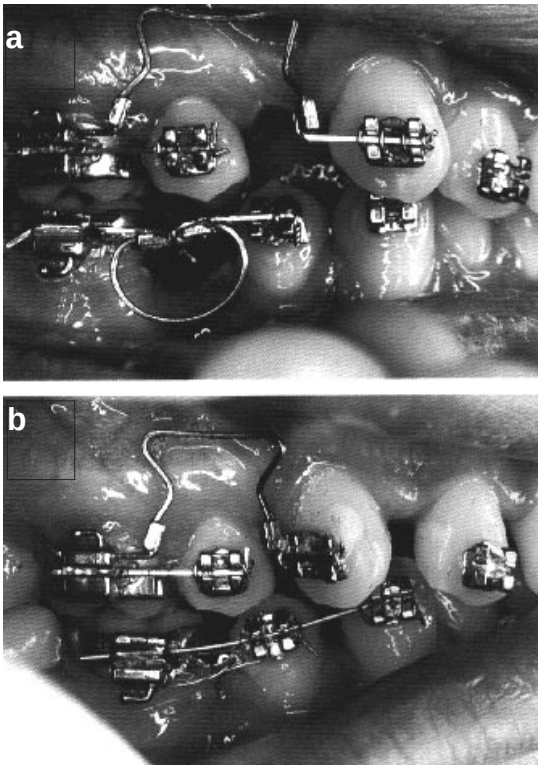

Figure 8 Example for the clinical application of a superelastic NiTi T-loop. (a) Initial intraoral situation. The tooth has to be translated over a distance of about 5 mm into the extraction site. An additional antirotation moment is produced by bending each steel arm by an angle of 30 degrees. (b) Treatment result after a period of about 3 months. Owing to an antitip moment that is slightly too small, the canine rotates about 5 degrees.

rates for all T-loops can be calculated. The value varies from 0.060 to 0.149 N/mm and is at least of a factor of three smaller than the force deflection rate of other retraction mechanisms. The overall mechanical characteristics of the superelastic T-loop indicate that it is suitable for clinical application.

Clinical application

Figure 8a and b shows a clinical application of the superelastic T-loop. The initial situation in Figure 8a shows that the canine should be moved into the extraction site on the left over a distance of about 4–5 mm without tipping or rotating it. The clinical result after a period of 4 months can be seen in Figure 8b. A total retraction of 5 mm was achieved, while the canine tipped and rotated by approximately 5 degrees. Owing to the broad range of activation and the low force/deflection rate, a second activation of the loop was not required. This satisfactory result indicates that the superelastic T-loop can be recommended for clinical application.

Discussion

The results obtained on the geometrical parameters of the loop were not influenced by the alloy. To this extent, the loop geometry can be produced with good quality and with a high reproducibility. Additionally, the wires can be heat treated without any influence on the mechanical parameters with temperatures up to 500°C (Miura *et al.*, 1986). This is confirmed by the present study and shows that heat treatment in an oven is an appropriate means for the production of superelastic orthodontic devices.

A more serious problem is the fact that all NiTi alloys display very different superelastic behaviour. Although a sample of wires from one distributor should have the same elasticity parameters, the properties differ from one batch to another and, even more so, the parameters may vary from one distributor to another. This influences the force systems of superelastic orthodontic devices significantly. The orthodontist has to check whether each individual batch is suitable for the production of a spring. Whilst the first produced spring might be suitable for an orthodontic application, the next one has to be rejected, although the calculated and measured force system of the underlying loop geometry was favourable.

Conclusions

The present study shows that orthodontic devices made of superelastic NiTi alloys provide mechanical characteristics that may not be reached with conventional alloys. The investigated superelastic T-loops generated nearly constant force systems over broad ranges of activation. However, the NiTi alloy used to construct the loops has a decisive influence on the measured force systems. Even a change in the batch of the same orthodontic NiTi wire results

in extreme changes in the force system of the retraction spring. Consequently, the manufacturers of superelastic NiTi alloys are asked either to keep the composition of their alloys constant in such a way that the mechanical properties of orthodontic NiTi wires remain unchanged, or to quantify the parameters of superelasticity for each individual batch. As the production of superelastic NiTi alloys is complicated and the mechanical behaviour of the alloy is extremely dependent on very small changes in composition, the latter would enable the orthodontist to decide whether the current batch is suitable for the planned treatment.

Address for correspondence

Dr. Christoph Bourauel
Department of Orthodontics,
University of Bonn
Welschnonnenstr. 17
D-53111 Bonn, Germany

Acknowledgements

This work was supported in part by grants from the Commission of the EU (BMH1-CT93-1712) and Deutsche Forschungsgemeinschaft (Dr196/1-1). The authors wish to thank the co-workers in the EU project 'Computer Aided Orthodontics' Dagmar Kobe (Bonn), Mike Dewar (London), Christopher Provatidis (Athens).

References

Andreasen G F, Brady P R 1972 A use hypothesis for 55 nitinol wire in orthodontics. Angle Orthodontist 42: 172–177

Andreasen G F, Hilleman T B 1971 An evaluation of 55 cobalt substituted nitinol wire for use in orthodontics. Journal of the American Dental Association 82: 1373–1375

Andreasen G F, Morrow R E 1978 Laboratory and clinical analyses of nitinol wire. American Journal of Orthodontics 73: 142–151

Andreasen G F, Bigelow H, Andrews J G 1979 55 Nitinol wire: force developed as a function of 'elastic memory'. Australian Dental Journal 24: 146–149

Bauer W, Diedrich P, Wehrbein H, Schneider B 1992 Der Lückenschluß mit T-Loops (Burstone)—eine klinische Studie. Fortschritte der Kieferorthopädie 53: 192–202

Bourauel C, Drescher D, Thier M 1992a An experimental apparatus for the simulation of three-dimensional movements in orthodontics. Journal of Biomedical Engineering 14: 371–378

Bourauel C, Nolte L P, Drescher D 1992b Numerische Untersuchung kieferorthopädischer Behandlungselemente aus pseudoelastischen NiTi-Legierungen. Biomedizinische Technik 37: 46–53

Bourauel C, Drescher D, Nolte LP 1993 Computergestützte Entwicklung kieferorthopädischer Behandlungselemente aus NiTi-Memory-Legierungen am Beispiel einer pseudoelastischen Retraktionsfeder. Fortschritte der Kieferorthopädie 53: 45–56

Buehler W J, Gilfrich J V, Wiley R C 1963 Effect of low-temperature phase changes on the mechanical properties of alloys near composition of TiNi. Journal of Applied Physics 34: 1475–1484

Burstone C J, Koenig H A 1974 Force systems from an ideal arch. American Journal of Orthodontics 65: 270–289

Burstone C J, Koenig H A 1976 Optimizing anterior and canine retraction. American Journal of Orthodontics 70: 1–20

DeFranco J, Koenig H, Burstone C J 1976 Three-dimensional large displacement analysis of orthodontic appliances. Journal of Biomechanics 9: 793–801

Drescher D, Bourauel C, Thier M 1991 Application of the orthodontic measurement and simulation system (OMSS) in orthodontics. European Journal of Orthodontics 13: 169–178

Gjessing P 1985 Biomechanical design and clinical evaluation of a new canine-retraction spring. American Journal of Orthodontics 87: 353–362

Gjessing P 1992 Controlled retraction of maxillary incisors. American Journal of Orthodontics and Dentofacial Orthopedics 101: 120–131

Greif R, Coltman M, Gailus M, Shapiro E 1982 Force generation from orthodontic appliances. Journal of Biomechanical Engineering 104: 280–289

Koenig H A, Burstone C J 1974 Analysis of generalized curved beams for orthodontic applications. Journal of Biomechanics 7: 429–435

Koenig H A, Vanderby R, Solonche D J, Burstone C J 1980 Force systems from orthodontic appliances: an analytical and experimental comparison. ASME Journal of Biomechanical Engineering 102: 294–300

Lipsett A W, Faulkner M G, El-Rayes K 1990 Large deformation analysis of orthodontic appliances. Journal of Biomechanical Engineering 112: 29–37

Miura F, Mogi M, Ohura Y, Hamanaka M 1986 The super-elastic property of the Japanese NiTi alloy wire for use in orthodontics. American Journal of Orthodontics and Dentofacial Orthopedics 90: 1–10

Miyakawa O, Shiokawa N, Matsuura T, Hanada K 1985 A new method for finite element simulation of orthodontic appliance–teeth–periodontium–alveolus system. Journal of Biomechanics 18: 277–284

Plietsch R, Bourauel C, Drescher D, Nellen B 1994 Analytical description of the bending behaviour of NiTi shape memory alloys. Journal of Materials Science 29: 5892–5902

Smith R, Storey E 1952 The importance of force in orthodontics. Australian Journal of Dentistry 56: 291–304

Solonche D J, Burstone C J, Vanderby R 1977 A device for determining the mechanical behavior of orthodontic appliances. IEEE Transactions of Biomedical Engineering 24: 538–539

Vanderby R, Burstone C J, Solonche D J, Ratches J A 1977 Experimentally determined force systems from vertically activated orthodontic loops. Angle Orthodontist 47: 272–279

Yang T Y, Baldwin J J 1974 Analysis of space closing springs in orthodontics. Journal of Biomechanics 7: 21–28